CLM-P831

Mathematical modelling of steam explosions

D. F. Fletcher
A. Thyagaraja

UK ATOMIC ENERGY AUTHORITY

Culham Laboratory

CLM-P831

Mathematical modelling of steam explosions

D. F. Fletcher and A. Thyagaraja

Culham Laboratory, Abingdon, Oxon, OX14 3DB, England

Abstract

In this paper we describe our work on the development of mathematical models of steam explosion phenomena. Most of the paper is concerned with describing a transient, two-dimensional, three-component model of coarse mixing. We present results illustrating the effect of varying the melt composition and of changing the initial conditions on the amount of coarse mixture produced. We also describe our recent work on the study of detonations and show the need to consider transient effects, rather than assuming a steady Chapman-Jouguet detonation.

October, 1987

Nomenclature

g	acceleration due to gravity
H	enthalpy
h	heat transfer coefficient
h_{fg}	latent heat of vaporization
L	length-scale
$\dot{m}$	volumetric source rate
P	pressure
$\bar{p}$	reduced pressure (defined in eq.5)
r	radial coordinate
T	temperature
t	time
U	radial velocity
V	axial velocity
z	axial coordinate

Greek symbols

α	volume fraction
ρ	density
χ	radial part of reduced pressure (defined in eq.5)
τ	timescale

suffixes

M	melt
S	steam
W	water

1. Introduction

Although steam explosions have been a subject for both theoretical and experimental study for many decades there are still a number of areas of uncertainty. It is believed that in most circumstances a steam explosion involves a progression through the stages of mixing, triggering, detonation and expansion [1]. However, many of the details of these processes remain uncertain. There is still no definitive answer to questions, such as, "How much melt will mix effectively in a given situation?" or "Will this mixture support a self-sustaining detonation?"

We have been involved in the development of mathematical models in an attempt to answer some of these questions. To date our work has been concerned mainly with modelling the initial coarse mixing stage. This has necessitated the development of a transient, two-dimensional, three-component multiphase flow code. A description of this model, together with a description of some of the calculations we have made with it, will constitute the bulk of this paper. Our current work is concerned with the development of a one-dimensional, transient detonation model. We will give a brief summary of our progress in this area and explain how our detonation model is related to our mixing work.

2. Coarse Mixing Modelling

2.1 Previous Work

In this section we will give a very brief review of previous work. Further details are given in reference 2. Limits to mixing are based on one of two different arguments. These invoke either dispersion of the mixture due to excessive steam production, or the failure of large diameter melt jets to be fragmented sufficiently to form a mixture. The latter area has been addressed theoretically by Theofanous and Saito [3] and Epstein and Fauske [4] and is currently being examined experimentally at Argonne National Laboratory (ANL) [5] and Sandia National Laboratory

(SNL) [6].

In this paper we will be concerned mainly with the first mechanism. Dispersion of the melt or liquid occurs because of the very large steam flows caused by rapid vapour production, due to the high temperature of the melt. Henry and Fauske [7] first proposed a very simple limit to mixing based on a Critical Heat Flux (CHF) criterion. This model is one-dimensional and steady. It assumes that mixing is limited to the amount of melt which gives rise to the same amount of vapour generation as that which would occur for the CHF from a flat plate heater with the same cross-section area as the mixing vessel. This model has been widely criticised because of its over-simplicity (see, for example, [2]).

Corradini and Moses [8,9] have attempted to improve upon this by producing a one-dimensional, transient model which uses data from the FITS experiments to avoid the need to solve the complex mass and momentum equations which govern mixing. Whilst this model provides considerable insight into the mixing process (in particular on the phenomena of melt and coolant sweep-out) it relies very heavily on experimental correlations and cannot be used to make predictions about other melt/coolant systems or conditions outside the range of its data-base.

The first attempt to model the transient mixing process in detail was made by Bankoff and co-workers, who developed a series of models based on the solution of multiphase flow equations for conservation of mass and momentum [10,11,12]. Their final model was transient, two-dimensional and assumed homogeneous flow of the water and steam. The melt was assumed to consist of spherical particles of a fixed size at a constant temperature. Model predictions showed that the melt was rapidly dispersed by the flow of vapour and there was little mixing for tonne scale melt pours.

Our work represents on extension of this model in that we allow for slip between all the phases and we have introduced a model of transient melt breakup. A similar approach is being pursued at Sandia with the

development of the IFCI code which can model all stages of a steam explosion [13]. Our strategy has been to develop separate models for each stage so that we can make use of special features, such as incompressible flow during mixing, to optimise our models and solution procedures. Furthermore, this step-by-step approach enables us, in principle, to validate each stage of the calculation with experiments (wherever possible). In the next section we will describe our model in detail.

2.2 Model Description

A complete description of the model is given in references 14 and 15. However, the main features of the model, together with the relevant conservation equations, will be presented here. We assume that mixing takes place axisymmetrically in a circular cylinder of radius R, height H, open at the top. The flow velocities are sufficiently small for us to assume incompressible flow so that the mass densities ρ_M, ρ_W and ρ_S may be taken as constant. We assume that the mixture consists of three components, melt (M), water (W) and steam (S). The water and steam are both assumed to be at their saturation temperature. With these assumptions it is possible to formulate the model in terms of a set of equations of the form

$$\frac{\partial}{\partial t}(\alpha_i \phi_i) + \frac{1}{r}\frac{\partial}{\partial r}(r U_i \alpha_i \phi_i) + \frac{\partial}{\partial z}(V_i \alpha_i \phi_i) = S_{\phi_i} \qquad (1)$$

where α_i is the volume fraction, U_i is the horizontal velocity and V_i is the vertical velocity of species i ($i = M,W,S$). Table 1 below lists the variables ϕ_i and the source terms for the water species equations, plus the melt enthalpy and melt length-scale equations. The equations and source terms for the other species are obtained by suitable permutation of the suffices.

Equation	ϕ	source term
Conservation of water mass	1	$\dot{m}_W/\rho_W$
Conservation of radial momentum	$\rho_W U_W$	$-\alpha_W \frac{\partial \bar{p}}{\partial r} - \alpha_W \frac{\partial \chi}{\partial r}$ $+F^r_{WM} + F^r_{WS} + F^r_{W\dot{m}}$
Conservation of axial momentum	$\rho_W V_W$	$-\alpha_W \frac{\partial \bar{p}}{\partial z} + g\alpha_W\alpha_M(\rho_M - \rho_W)$ $+g\alpha_W\alpha_S(\rho_S - \rho_W)$ $+F^z_{WM} + F^z_{WS} + F^z_{W\dot{m}}$
Melt enthalpy	$\rho_M H_M$	$-\dot{m}_S h_{fg}$
Melt length-scale	L_M	$-\alpha_M(L_M - L_{crit})/\tau_L$

Table 1 : Coefficients and source terms for some of the conservation equations.

In addition to the above equations the volume fractions must satisfy the constraint

$$\alpha_M + \alpha_W + \alpha_S = 1 \qquad (2)$$

which implies the following elliptic constraint,

$$\frac{1}{r}\frac{\partial}{\partial r}\left(r(\alpha_M U_M + \alpha_W U_W + \alpha_S U_S)\right)$$

$$+ \frac{\partial}{\partial z}(\alpha_M V_M + \alpha_W V_W + \alpha_S V_S) = \frac{\dot{m}_S}{\rho_S} - \frac{\dot{m}_W}{\rho_W} \qquad (3)$$

The above equation allows the common pressure to be determined, as will be illustrated later.

It now only remains to describe the source terms, together with the necessary constitutive relations needed to close the problem. We assume that there are no sources or sinks of melt inside the vessel so that $\dot{m}_M = 0$. Melt is usually injected at the top boundary. Since the water and steam are assumed to be saturated there is no condensation of steam (ie $\dot{m}_S \geq 0$). Conservation of mass gives $\dot{m}_W = -\dot{m}_S$ and we set

$$\dot{m}_S = \alpha_W \alpha_M 6h\ (T_M - T_W)/L_M\ h_{fg} \qquad (4)$$

where we have assumed the melt to be in the form of spheres of diameter L_M. T_M and T_W are the melt and water temperatures, h_{fg} is the latent heat of vaporization and h is the appropriate surface heat transfer coefficient. In our calculations we have assumed that h is the sum of a gray body radiation term and a convective film boiling term. The convective film boiling correlation of Witte [16] was used.

The term α_W on the r.h.s. of equation (4) ensures that vapour production only occurs when there is water present. The choice of a factor linear in α_W is arbitrary. The heat transfer processes within a mixture are very complex. Because of the high temperature of the melt the absorbtion length of water is long (for melt at 3400K only 60% of the radiation energy is absorbed in 30mm of water [17]). In addition, the melt starts out by being in film boiling in water but so much steam is produced

that the continuous phase becomes vapour and the heat transfer rate is reduced. These ideas are explored in more detail in reference 17. It is sufficient to note here that the form of the source term in our code can be readily modified to account for our improved understanding as more experimental data becomes available.

In the momentum equations we work with a reduced pressure, defined by

$$\bar{p} = p - \chi = p - \int_z^H g(\alpha_M \rho_M + \alpha_W \rho_W + \alpha_S \rho_S) dz \qquad (5)$$

Thus the usual axial momentum source term $-\alpha_W \frac{\partial p}{\partial r} - \alpha_W \rho_W g$ takes the form given in table 1 and $\frac{\partial \chi}{\partial r}$ terms appear in the radial momentum equations. The introduction of a reduced pressure greatly improves the stability and convergence properties of the pressure correction scheme used to solve the equations.

The terms F^r_{WM} and F^z_{WM} represent interphase drag between the melt and water in the r and z directions respectively. These terms have been modelled using a general drag law proposed by Harlow and Amsden [18] and their exact form is given in reference 14. The important point to note is that

$$F^r_{WM} \equiv D^r_{WM}(\alpha_M, \alpha_W, L_M, L_W, U_M, U_W, V_M, V_W)(U_M - U_W) \qquad (6)$$

so that provided $D^r_{WM} = D^r_{MW}$ Newton's third law is satisfied. There is a lack of experimental data on the drag force in three component mixtures of the type encountered in the study of coarse mixing. Experimentally it is very difficult to determine exactly what a mixture consists of and it is even more difficult to measure the transient drag forces. Thus we have chosen to use a very general drag law which can easily be modified or replaced as improved experimental data become available. Other drag laws are examined in [17].

The terms $F^z_{\dot{W}m}$ and $F^r_{\dot{W}m}$ represent evaporation reaction forces and are not present in the melt equation. These take the form

$$F^r_{\dot{W}m} = -\dot{m}_S U_W \ , \quad F^r_{\dot{S}m} = \dot{m}_S U_W \tag{7}$$

In the enthalpy equation the kinetic energy of the melt and terms arising from pressure and drag work have been neglected, since they are small compared with the thermal energy terms. The source term ensures that the melt cools by an amount consistent with the heat used to produce vapour. The melt temperature is determined from the enthalpy by using a suitable caloric equation of state. Energy equations are not required for the steam and water phases as they are both assumed to be at their saturation temperature.

In the melt length-scale equation the source term causes the melt length-scale to reduce to L_{crit} with a fragmentation time of τ_L. The choice of a model for L_{crit} and τ_L is complicated by uncertainties over the breakup mechanism and the choice of appropriate effective fluid surrounding the melt drops. To date we have used constant values for L_{crit} and τ_L. Work is underway at Sandia to develop breakup correlations valid for both small droplets and large jets based on the analysis of experimental data [13]. As further data becomes available we can easily modify our model. In addition, it is a simple matter to introduce conservation equations for both the steam and water length-scales but at present, in our view, there is insufficient experimental data to warrant their use.

2.3 Boundary and Initial Conditions

We set the normal velocity component to zero on all solid boundaries. Since there is no viscosity in the model we do not implement a no-slip boundary condition. At the top (z = H) we set the radial velocity of all the components to zero and set the vertical gradient of V_W and V_M to zero.

A uniform steam velocity outlet profile is assumed with the flow rate determined from the volume integral of equation (3).

In incompressible flow pressure is a relative variable so that at the exit plane we set $\bar{p} = 0$ at one point to fix its level and determine the remainder of the pressure field during the course of the solution. At $t = 0$ an initial velocity and volume fraction field is specified together with the length-scale and temperature of each species. Any melt injected into the solution domain is given a specified velocity, length-scale and enthalpy.

2.4 Solution Procedure

Only the outline of the solution procedure is presented here as full details are given in reference 14. The equations were finite differenced using a staggered grid. Upstream differencing was used for convective terms for stability. The solution procedure is as follows:

(a) Time advance the α_M equation to get $\alpha_M(t + \Delta t)$ using the melt velocity and α_M fields at time t.

(b) Similarly time advance L_M and H_M and determine T_M using the caloric equation.

(c) Time advance the α_W equation treating the source term implicitly.

(d) Determine $\alpha_S = 1 - \alpha_W - \alpha_M$.

(e) Determine the new velocity fields using the pressure field at time t.

(f) Substitute the new velocity and volume fraction fields into the finite differenced form of equation (3) to determine the local continuity error.

(g) If this error is too large, update the pressures using Newton's method, go back to step (e) and repeat the procedure using the latest pressure field. Iterate steps (e) → (g) until the local continuity errors (suitably normalised) are below the desired accuracy level.

Typically after 2 iterations the above procedure converges and the code steps forward in time again. The chosen method of time advancing the α's ensures that they remain positive and if the continuity error is reduced to a suitably small value they remain less than unity [19]. For stability we require the Courant number (Max $(\frac{V_i \Delta t}{\Delta z}, \frac{U_i \Delta t}{\Delta r})$) to be less than unity and for accuracy we require the product of any rate parameters and the time-step to be less than unity e.g. $\Delta t/\tau_L << 1$.

In the momentum equations the velocities of all the species are coupled at each grid location due to the drag terms. Thus at each grid point we invert a 3 x 3 matrix to obtain the new velocities of all 3 species simultaneously. This procedure ensures that Newton's third law is exactly satisfied. The pressure correction is carried out by first correcting the pressure level in vertical blocks and then correcting the pressure within the blocks. This procedure avoids the need to solve the full 2-D Poisson's equation and instead we use a TDMA solution for the block correction and then a TDMA solution within each block.

2.5 Model Validation

The code has been tested extensively on model problems and has been found to give grid independent solutions which depend continuously on the initial data. It has been used to simulate the one-dimensional experiments carried out at Brookhaven National Laboratory [20] in which heated ball bearings were dropped into water [21]. It has also been used successfully to simulate the ANL experiment (CWTI-9) [22] in which a corium jet was injected into a pool of water [14,15]. In addition, it has been used to examine the effect of pressure on mixing [21] and to examine the role of vapour production [14]. Unfortunately there is very little

data available which is entirely suitable for modelling purposes as it is important to have both well-defined initial conditions and reasonably detailed transient measurements to make experimental comparison worthwhile. We will present some further simulations in section 3 of this paper in which we will examine the effect of changing the melt material and examine the effect of radial spreading of the melt jet.

2.6 A Quantitative Measure of Mixing

The code enables us to calculate the evolution of the volume fractions, the melt lengthscale etc and a typical run produces an enormous amount of data. If we had a complete model of the steam explosion process we would be able to stop the mixing calculation and examine the potential for a detonation by introducing a pressure pulse to trigger the mixture. Our aim is to produce a detonation model to enable us to determine which mixtures can support the escalation of a localized interaction into a propagating detonation. As an interim measure and to gain some insight into the dynamical evolution of a mixture we have produced a qualitative measure of mixing. This measure contains qualitatively, in our view, the current state of knowledge of what constitutes a "good" mixture. For example, both melt and water must be present, there must not be too much steam and the melt particle size must not be too large. A full description of the chosen function is given in reference 23 but it will be summarised briefly here for completeness. We set

$$\theta = 16\ \alpha_W \alpha_M (1 - \alpha_W)(1 - \alpha_M)\ f(\alpha_S)\ g\ (L_M) \qquad (8)$$

The function θ takes values between zero and one and attains its maximum value when the mixture consists of equal volumes of melt and water. The functions $f(\alpha_S)$ and $g(L_M)$ are unity except when either $\alpha_S > \alpha_{crit}$ or $L_M > L_{MCRIT}$ in which case they tend rapidly to zero. These two functions account for the fact that detonations are inhibited if there is too much vapour or the melt particles are too large. Typically we set $\alpha_{crit} = 0.6$ and $L_{MCRIT} = 10\text{mm}$.

The function allows us to compare different simulations and to

determine an approximate region of mixture in each case. Now that the model, together with a means of describing a mixture, have been described we will present the results of some simulations.

3. Mixing Simulations

In this paper we present the results from two sets of simulations of coarse mixing. The first series compares the mixing of three different melts with water. The second series examines the effect of jet spreading on the mixing process. We use the same geometry and finite difference grid in each case. The vessel geometry is shown in figure 1. We used a 10×10 finite difference grid and a time-step of 10^{-5}s. Each simulation were carried out for an ambient pressure of 0.1MPa. All the length-scales were assumed to be fixed and values of L_M = 5mm, L_S = 20mm and L_W= 20mm were used and all the drag coefficients were set to 0.2. In the base case calculation 41kg of UO_2 was injected with a vertical velocity of 3m/s and a pour diameter of 100mm. The vessel contained 460kg of water.

3.1 The Effect of Melt properties

We carried out 3 simulations using identical volumes of melt for melts of uranium dioxide, steel and aluminium. The important differences in physical properties are given in Table 2 below.

Property	UO_2	Steel	Al
Initial Temperature (K)	3400	2000	1200
Freezing Temperature (K)	3120	1730	933
Density (kg/m^3)	8,400	6,900	2,700
Latent heat (J/kg)	2.77×10^5	2.7×10^5	3.95×10^5
Heat capacity (J/kgK)	503	600	1070
Emissivity	0.84	1.0	0.4

Table 2: Melt Properties

In all cases the melt superheat was approximately 270K.

Figure 2 shows a comparison of the transient steaming rate for the three different melts. The figure shows that there is a considerable difference in the steaming rate with very different behaviour being shown in the UO_2 simulation compared with the other two simulations. In the UO_2 case the steaming rate rapidly rises to 8kg/s as the melt enters the water and then falls rapidly as the steam production causes the mixture to be dispersed. In the case of steel and aluminium there is a much slower rise to a lower peak value and then steam production remains constant for approximately 0.3s.

The differing steam production rates cause different amounts of sweep-out from the vessel in the various cases. For the UO_2 case 3% of the melt and 36% of the water is swept-out after 0.5s. In the case of steel 1% of the melt and 0.2% of the water is lost and in the case of aluminium the loss is negligible. The exact value of the masses of material swept-out obviously depends on the chosen form of the drag law and is simplified in this case because we have chosen fixed length-scales. However, the calculation does illustrate the considerable difference between the behaviour of the different melts.

Examination of the melt temperature fields showed that after 0.5s there was little cooling of the melt in the bulk of the mixture but that around the edges where the mixture was very dispersed the UO_2 has cooled by approximately 270K, the steel by 150K and the aluminium by 20K. These figures are consistent with the vapour production data and show that a significant error would not be introduced by assuming a constant temperature. In the dispersed zone the UO_2 was approaching its freezing temperature.

The differences between the coarse mixtures produced are best illustrated by using the mixing index described in section 2.6. Figures 3(a) (b) and (c) show contour plots of θ for the three different melts 0.2s after the start of melt injection. The effect of vapour production on mixing is clearly illustrated. The mixture produced in the case of UO_2

is much more dispersed than in the other two cases. In the case of UO_2 the mixture region consists of a paraboloid of revolution surrounding a central core of mixture. This is qualitatively very similar to the shape of the mixture region observed in some of the FITS experiments [24]. The steel and aluminium cases are similar to each other, but with better mixing in the aluminium case. The different locations of the zones of mixture is due to the different densities of the melt causing different fall velocities. The figures show very clearly the different nature of the mixture when it reaches the vessel base at which time triggering is likely to occur [25]. The data presented here shows that care must be taken in making conclusions about one system from data collected from a different one.

3.2 The Effect of Jet Spreading on Mixing

In this section we present the results of a series of calculations carried out to examine the effect of jet spreading on mixing. This topic is of particular interest since jet breakup is currently a topic of experimental investigation at various laboratories [5,6]. We used almost the same geometry as described in the previous section. The only difference was that the large area pour of melt was replaced by a 50mm diameter jet of UO_2 and the pouring time was increased to 0.2s so that the same mass of melt was injected. We examined three different cases: a jet with no initial radial velocity and jets with initial radial velocities of 0.2m/s and 0.6m/s.

The steaming rate for each of these cases is shown in Figure 4. The figure shows that increasing the initial jet spreading rate increases the steam production rate. This is because the melt is spread radially so that more melt contacts the water. In the case of the 0.6m/s initial velocity vapour production disperses the mixture after about 0.3s and the steam production rate falls. Also shown as a dotted line is the steam production rate for the case of a wide jet (without an initial radial velocity) described in section 3.1. The figure shows that the two different initial conditions lead to very different steam production

transients.

The different vapour production rates lead to very different amounts of melt and water sweep-out. Increasing the radial velocity increased the sweep-out of melt from 10% for U = 0, to 22% for U = 0.2m/s and to 70% for U = 0.6m/s. Increasing the radial velocity had the opposite effect on the sweep-out of water with 32% being swept-out for the case U = 0 and virtually no water being lost in the other two cases. These results again illustrate the sensitivity of the mixing process to the initial conditions.

Figure 5 shows the mixture function for the case of no initial radial velocity and an initial radial velocity of 0.6m/s. The plot shows clearly the dispersive effect of the radial velocity. The mixture is very different in character in the two cases. In the case with no radial velocity there is a central core containing a "good" mixture whereas in the case with an initial radial velocity the centre of the mixture zone is filled with steam. Apart from the differences in shape, it would be impossible to distinguish between the two cases in experiments by using optical means alone. This type of simulation highlights the need for sophisticated experimental means of probing the inside of a mixture to determine how well simulations describe real mixtures.

Comparison of figure 5a with figure 3a shows the effect of changing the jet diameter for a fixed mass of melt injected. The mixing zone is much more compact in the case of a narrow jet. This is because steam production is reduced by the close packing of melt (see figure 4) and thus the mixture is not dispersed so rapidly.

3.3 Summary of Mixing Results

The results presented here together with those presented in our earlier work clearly show that steam production plays a very important part in the evolution of a mixture. The calculations demonstrate that low temperature simulants can produce regions of very good mixture in

situations where high temperature melts, such as UO_2, do not.

Figure 6 shows the water volume fraction contours for the wide jet pour of UO_2 0.25s after the start of the calculation. The figure shows that vapour production is so rapid that it completely disperses the water overlying the mixture zone. This phenomena could be very important in reducing the violence of an explosion as steam produced in the detonation stage of the explosion would vent into the overlying region of low pressure gas. Steam chimneys similar to this were observed in the FITS experiments [24,26]. Calculations presented by Corradini [26] show that in some circumstances shock waves generated in the detonation process are able to close this region up. A thorough study of this phenomena is needed, however, before it becomes clear whether efficient explosions can occur in situations where the overlying water pool is highly voided.

For the situation shown in figure 6 the steam velocity was of the order of 75m/s in the centre of the mixing zone and the water velocity was of the order of 3m/s. This shows that the assumption of homogeneous flow of water and steam is not reliable in these conditions where vapour production is so rapid.

Of course, it should be borne in mind that the mixing index we have been using in this work is only an approximation in the absence of reliable data of what constitutes a "good" mixture. In the next section we will describe our approach to the development of a detonation model which will enable us to determine what mixtures can sustain a propagating detonation wave.

4. Detonation Modelling

In this section we give a brief summary of our detonation work. Numerous workers [27,28] have developed steady-state models of detonations based on the Board-Hall model [29] where the analogue between steam explosions and chemical detonations was first examined. Steady-state models assume that the explosion zone is terminated by a Chapman-Jouguet plane at which the flow is just sonic relative to a frame of reference

moving with the detonation front. Whilst there can be little doubt that the C-J condition is required for a steady-state solution of the equations to exist, it is by no means obvious that there is sufficient time available for a steady-state solution to develop in any particular application. We aim to overcome these problems by carrying out a transient simulation in which a pressure pulse is incident upon a region of coarse mixture. This will allow us to examine escalation and decay of detonations as well a steady-state propagation.

To date we have modelled systems which consist of only two-components, namely a 'burnt' and 'unburnt' fluid. Our work has been concerned with the formulation of a one-dimensional multiphase flow model based on the usual multiphase flow equations. The numerical scheme we have developed is reported in references 30 and 31, together with a number of test cases. In the work reported in reference 32 we have used this system of equations to examine the effect of initial conditions and constitutive relations on the form of the solution obtained. This has enabled us to test the model thoroughly and to make several interesting observations.

Firstly, our calculations have shown that for a wide range of initial conditions and trigger mechanisms (e.g. combustion only occurs when a critical pressure or temperature is exceeded in the 'unburnt' fluid) the C-J condition may not be approached for a considerable time. Thus in problems of practical interest walls may be encountered before the detonation process has reached a steady-state. Secondly, we have observed that depending on the trigger threshold we may generate strong or weak detonations. Figures 7 and 8 show typical examples of strong and weak detonations. In the strong detonation case a high pressure or temperature was required to be exceeded before combustion was initiated. Because of the high trigger pulse used, a strong detonation was initiated and has travelled a considerable distance without being weakened to form a C-J detonation. In contrast, in the case of the weak detonation only a small increase in pressure or temperature was needed to cause "combustion" and the detonation wave develops and approaches the C-J point from below.

Full details of the simulations are given in reference 32.

There is insufficient space in the present paper to describe all the results obtained using our two-component detonation model. However, the above examples highlight the importance of modelling transient effects and illustrate the type of solutions obtained from the model. Our future work will be concerned with modelling the more complex situation of interest in steam explosion research in which melt is fragmented and transfers its heat to the surrounding water/steam mixture. This will not introduce any further mathematical complications but the problem of finding suitable constitutive relations is again formidable. For a definitive resolution of these issues there is a need for both well instrumented experiments to determine constitutive relations and for integral experiments to allow model comparison to be made.

Studies carried out at the University of Stuttgart [33] using both transient and steady-state detonation models support these ideas. These authors also suggest the need to examine the possibility of the existence of strong detonations and have observed that a very long region of mixture (~2m in some cases) is needed to achieve steady-state propagation. In their numerous publications (referred to in [33]) they have identified the need for both of the types of experiments described above to verify the constitutive relations and the final model.

5. Conclusions

In this paper we have described two areas in which mathematical models have been used to examine different aspects of the steam explosion phenomenon. We have developed a coarse mixing model which enables the influence of the flow of steam on mixing to be examined in situations of engineering interest. This mechanism is invoked in most limits-to-mixing arguments. We have also briefly described a transient model of detonations and illustrated the importance of considering transient effects.

The work presented in this paper and contained in much of the

literature cited shows that sophisticated mathematical models of the steam explosion process can be solved using the modern generation of super computers. This work highlights the need for good quality experimental data both in order to determine the appropriate constitutive relations for mechanisms, such as drag and fragmentation and for integral experiments to validate the models. The theoretical models presented are capable of stimulating novel experimental work which can, in turn, lead to improved predictive techniques. Fundamental progress in this area can only be expected if there is a fruitful interaction between theory and experiment as outlined above.

Acknowledgements

The authors would like to thank Mrs. E. Barnham and Mrs. G.M. Lane for their careful preparation of this manuscript.

References

1. A.W. Cronenberg, Recent developments in the understanding of energetic molten fuel-coolant interactions. Nucl. Safety, 21, 319-337, (1980).

2. D.F. Fletcher, A Review of coarse mixing models. Culham Laboratory Report: CLM-R251, (1985).

3. T.G. Theofanous and M. Saito, An assessment of class-9 (core melt) accidents for PWR dry containment systems. Nucl. Eng. Des., 66, 301-332, (1981).

4. M. Epstein and H.K. Fauske, Steam film instability and the mixing of core-melt jets and water. Proc. National Heat Transfer Conf., Denver, August, (1985).

5. B.W. Spencer, J.D. Gabor and J.C. Cassulo, Effect of boiling regime on melt stream breakup in water. Proc. 4th Miami Int. Symp. Multiphase transport and particulate phenomena, Miami beach, Florida, 15-17 December, (1986).

6. B.W. Marshall, M.Berman and M.F. Young, Jet mixing experiments. In Reactor Safety Research Semi-annual Report Jan-Jun, 1986, NUREG/CR-4805(1) (1987).

7. R.E. Henry and H.K. Fauske. Required initial conditions for energetic steam explosions. Paper presented at the ASME winter meeting, Washington, (1981).

8. M.L. Corradini and G.A. Moses. A dynamic model for fuel-coolant mixing. Proc. Int. meeting on Light Water Reactor Severe Accident Evaluation, Cambridge, Massachusetts, (1983).

9. M.L. Corradini and G.A. Moses, Limits to fuel/coolant mixing. Nucl. Sci. Eng., 90, 19-27, (1985).

10. S.G. Bankoff and S.H. Han, Mixing of molten core material and water. Nucl. Sci. Eng., 85, 387-395, (1983).

11. S.H. Han and S.G. Bankoff, An unsteady one-dimensional model for fuel-coolant mixing in an LWR meltdown accident, Nucl. Eng. Des., 95, 285-295, (1986).

12. S.G. Bankoff and A. Hadid, The application of a user-friendly code to nuclear thermal hydraulic reactor safety problems. Paper presented at the Int. Nuclear Power Plant Thermal Hydraulics and Operations Meeting, Taipei, Taiwan, ROC, 22-24 October, (1984).

13. M. Berman and M.F. Young, Private communication, (1987).

14. A. Thyagaraja and D.F. Fletcher, Buoyancy-driven, transient, two-dimensional thermo-hydrodynamics of a melt-water-steam mixture. Comput. Fluids, 16, 59-80, (1988).

15. D.F. Fletcher and A. Thyagaraja, Numerical simulation of two-dimensional transient multiphase mixing. Proc. 5th Int. Conf. for Numerical Methods in Thermal Problems, Montreal, Canada, June 29th-July 3rd 1987, V (2), 945-956, Pineridge, (1987).

16. L.C. Witte, Film boiling from a sphere. I and EC Fundamentals, 7, 517-518, (1968).

17 D.F. Fletcher, Assessment and development of the Bankoff and Han coarse mixing model. Culham Laboratory Report: CLM-R252, (1985).

18. F.H. Harlow and A.A. Amsden, Flow of interpenetrating material phases. J. Comp. Phys., 18, 440-465, (1975).

19. A. Thyagaraja, D.F. Fletcher and I. Cook, One dimensional calculations of two-phase mixing flows. Int. J. Numer. Methods Eng., 24, 459-469, (1987).

20. G.A. Greene, T. Ginsberg and N.K. Tut, BNL severe accident sequence experiments and analysis program. In proc. 12th NRC water reactor information meeting, Gaitisburg, 1984, 3, (1985).

21. D.F. Fletcher and A. Thyagaraja, Numerical simulation of one-dimensional multiphase mixing. Culham Laboratory Report: CLM-P776, (1986).

22. B.W. Spencer, L. Mcumber, D. Gregorash, R. Aeschlimann and J.J. Sienicki, Corium quench in deep pool mixing experiments. Proc. National Heat Transfer Conf., Denver, August, (1985).

23. D.F. Fletcher and A. Thyagaraja, A method of quantitatively describing a multi-component mixture. PhysicoChem. Hydrodynam., 9, 621-631, (1987).

24. Berman, M, (ed.) Light water reactor safety research program semi-annual report, October 1981 - March 1982. NUREG/CR-2841, 1982.

25. G. Long, Explosions of molten metal in water - causes and prevention. Metals Progress, 71, 107-112, (1975).

26. M.L. Corradini, Analysis and Modelling of Large-scale steam explosion experiments. Nucl. Sci. Eng., 82, 429-447, (1982).

27. A. Sharon and S.G. Bankoff, On the existence of steady supercritical plane thermal detonations. Int. J. Heat Mass Transfer, 24, 50-61, (1981).

28. E. Scott and G. Berthoud, Multiphase thermal detonations. Topics in two-phase heat transfer, (ed. S.G. Bankoff), ASME, New York, (1978).

29. S.J. Board, R.W. Hall and R.S. Hall, Detonation of fuel coolant explosions. Nature, 254, 319-321, (1975).

30. D.F. Fletcher and A. Thyagaraja, Some calculations of shocks and detonations for gas mixtures. Culham Laboratory report: CLM-R276, (1987).

31. D.F. Fletcher and A. Thyagaraja, Multiphase flow simulations of shocks and detonations, Part 1: Mathematical formulation and shocks. Culham Laboratory report: CLM-R279, (1987).

32. A. Thyagaraja and D.F. Fletcher, Multiphase flow simulations of shocks and detonations, Part II: Detonations. Culham Laboratory report: CLM-R280, (1987).

33. C. Carachalios, M. Bürger and H. Unger. The thermal detonation theory in comparison with large scale vapour explosion experiments. Proc. Int. ANS/ENS Topical Meeting on Thermal Reactor Safety, San Diego, California, U.S.A., February 2-6, Vol. I, paper II.1, (1986).

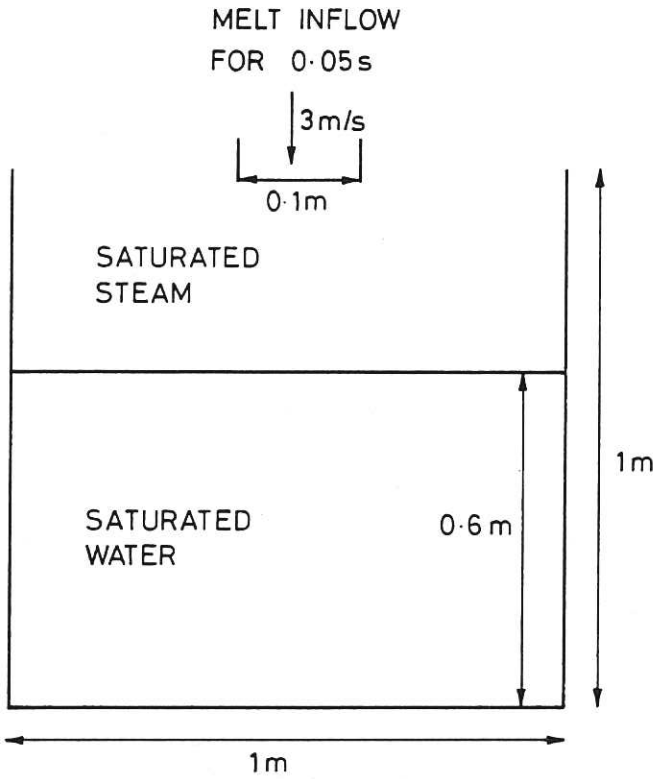

Fig. 1 Vessel Geometry

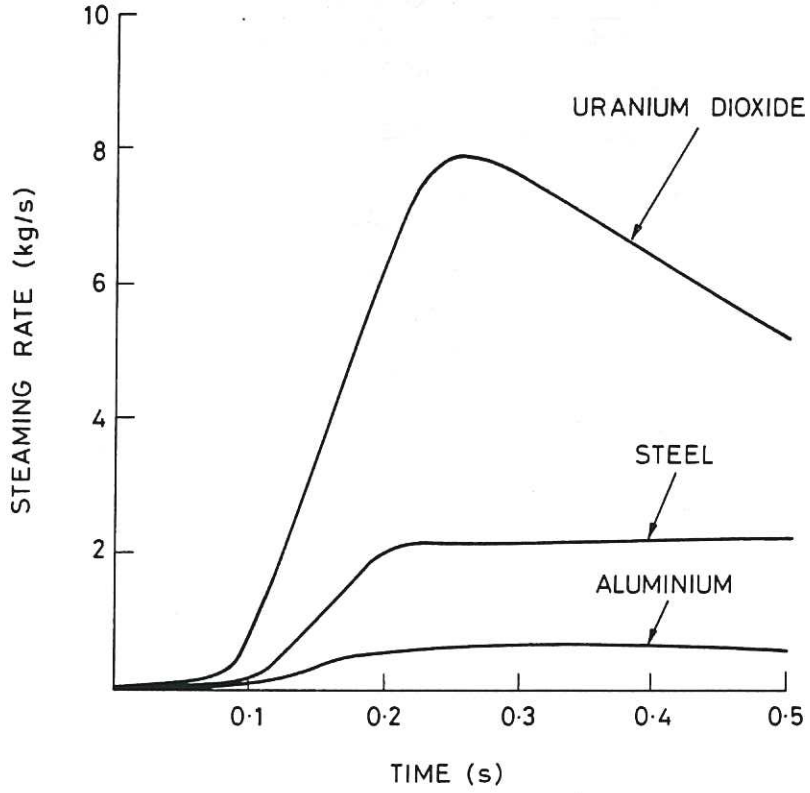

Fig. 2 The transient steaming rate for various melts.

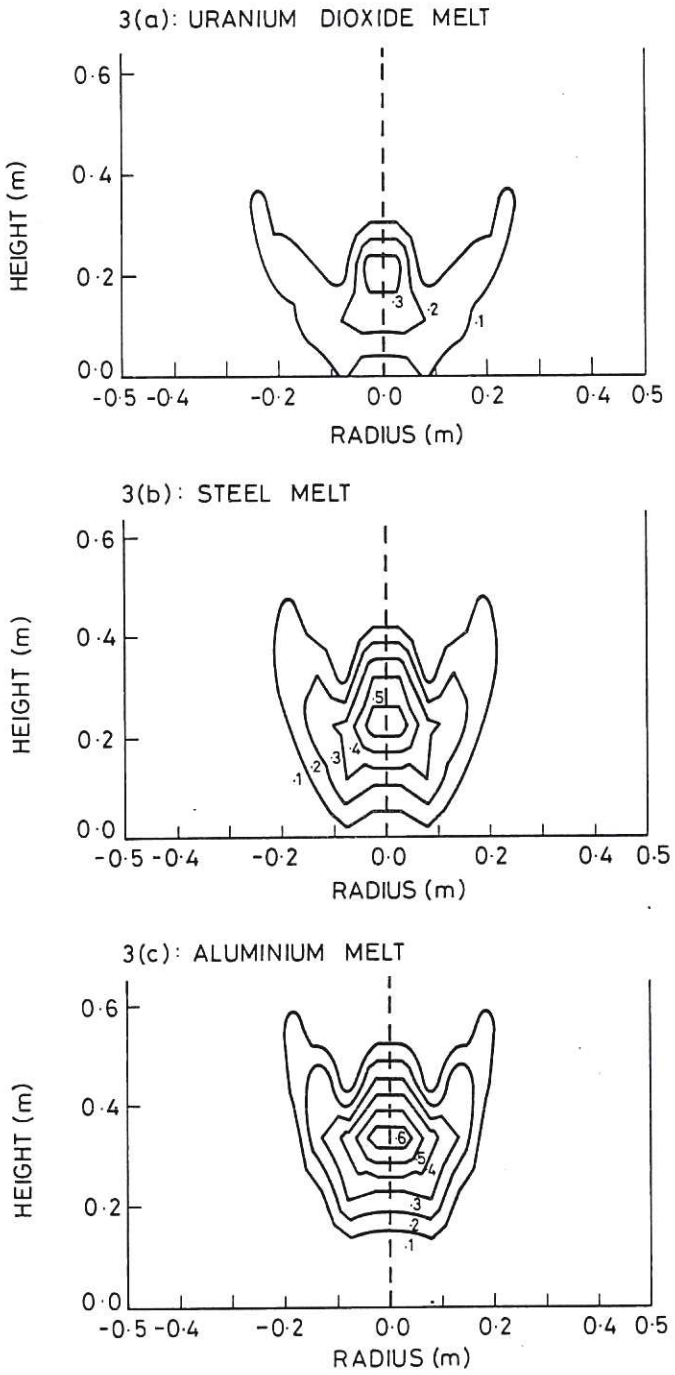

Fig. 3 Mixture function 0.2s after pouring for various melts.

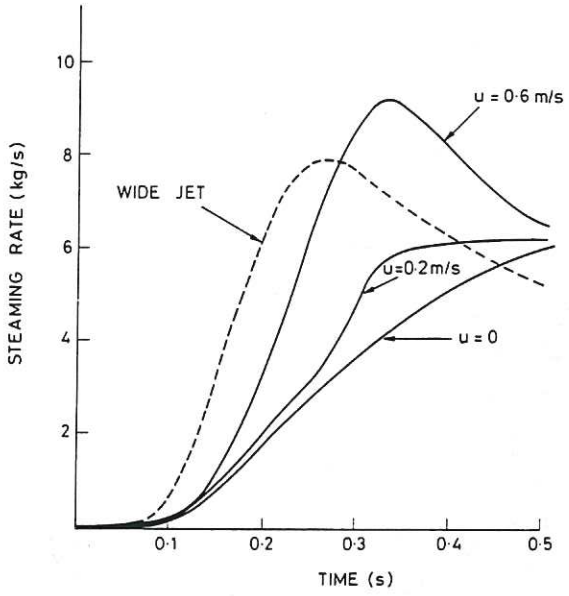

Fig. 4 The effect of melt pour conditions on the transient steaming rate.

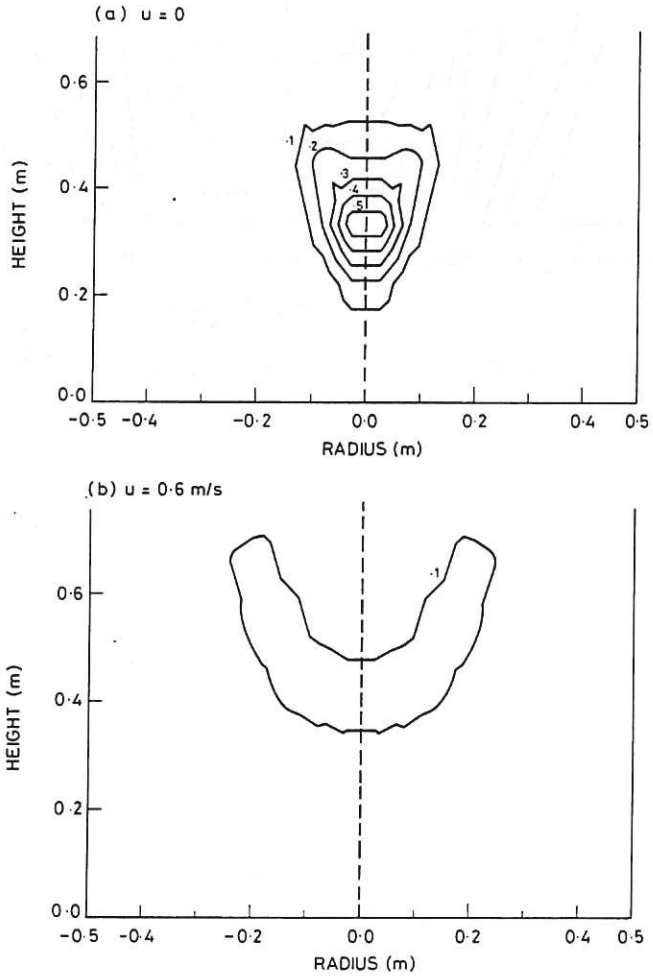

Fig. 5 Mixture function 0.2s after pouring for various initial conditions.

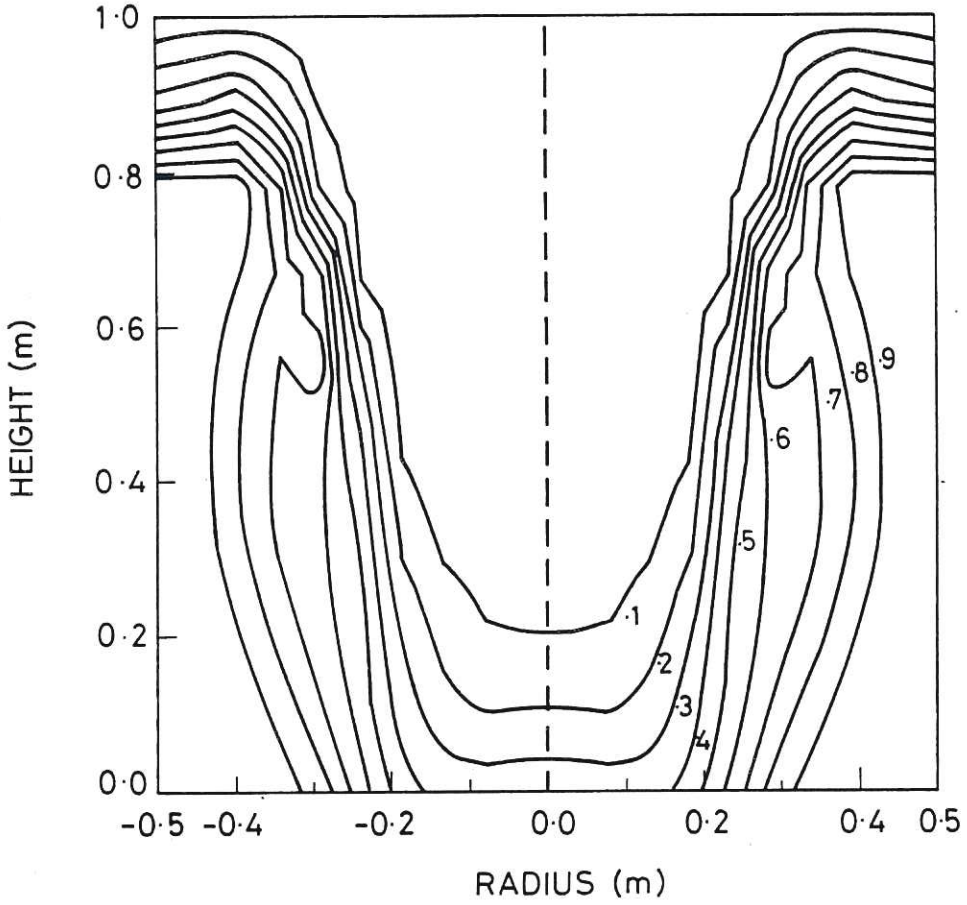

Fig. 6 Water volume fraction contours showing the vapour chimney above the mixing zone.

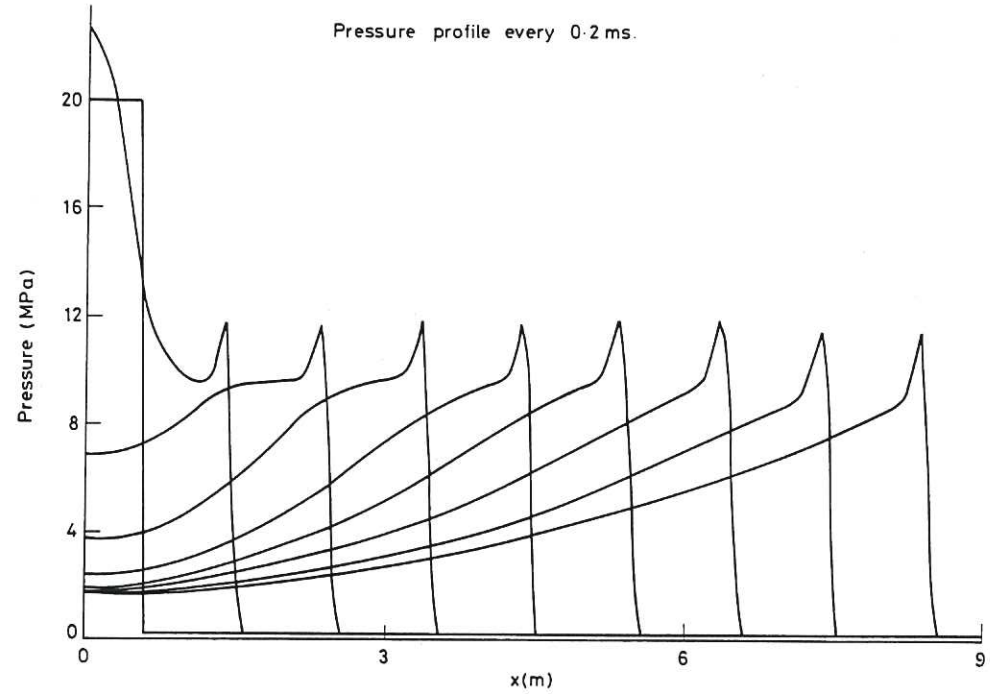

Fig. 7 Pressure profile for a strong detonation.

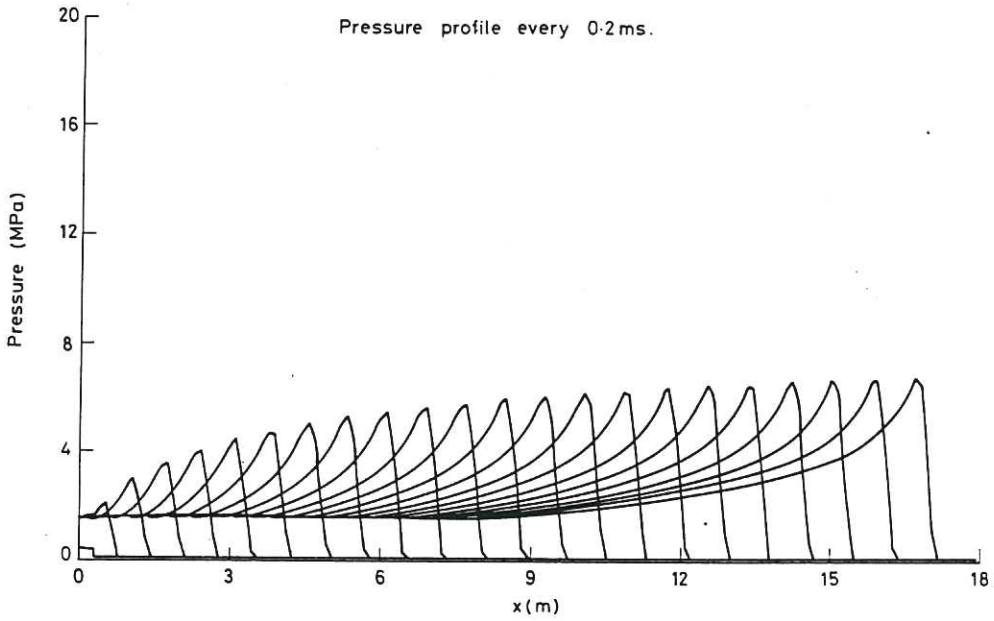

Fig. 8 Pressure profile for a weak detonation.